

## PHBV/cellulose nanofibrils composites obtained by solution casting and electrospinning process

Kelly C. C. de Carvalho Benini<sup>1</sup>, Maria Odila Hilário Cioffi<sup>1</sup>  
Herman Jacobus Cornelis Voorwald<sup>1</sup>

<sup>1</sup> Unesp – São Paulo State University, Department of Materials and Technology (DMT), Fatigue and Aeronautical Materials Group, CEP: 12.516-410, Guaratinguetá, SP  
e-mail: kcccarvalho@hotmail.com

### ABSTRACT

In this work, nanobiocomposites of poly (3-hydroxybutyrate-co-3-hydroxyvalerate) (PHBV) reinforced with cellulose nanofibrils (CNFs) were produced by electrospinning and solution casting process. CNFs were obtained by sulfuric acid hydrolysis from *Imperata brasiliensis* fibers. Nanocomposites loaded with 1 (wt. %) of CNFs were prepared using a mixture of solvents chloroform (CHCl<sub>3</sub>): N, N-dimethylformamide (DMF), in the ratio of 78:22 with 30 h of solubilization. Films by solution casting were obtained in a petri dish, at 50 °C for 1 hour, using drying casting temperature of 153 °C. Mats by electrospinning were obtained with a needle 20x10, drum collector rotation 27 rpm, and working distance of 10 cm. Films and mats were characterized by Scanning Electron Microscopy (SEM), X-ray diffraction (XRD) and Differential Scanning Calorimetry (DSC). It was possible to conclude that for nanobiocomposites obtained by solution casting, the addition of CNFs did not affect the transparency of the films, but provided a significant increase in the crystallization rate as observed by DSC analysis, while for electrospinning nanobiocomposites a considerable improvement in process increasing electrospinning time and quality of the mats manufactured, were observed.

**Keywords:** cellulose nanofibrils, PHBV, electrospinning, solution casting.

### 1. INTRODUCTION

The properties of nanobiocomposites, compared to conventional one, are extensively studied by presenting many advantages such as better recyclability, transparency, low weight and superior thermal, mechanical and barrier properties, at low reinforcement levels (less than 10%) [1, 2].

The use of cellulose nanofibers as reinforcement for biodegradable matrixes have attracted the attention of many researchers because both reinforcement and matrix are derived from renewable and biodegradable sources [3]. The effect of the nanocellulose addition on the polymeric matrix depends on the properties of nanocellulose such as size, morphology, crystalline structure and others, which vary according to extraction source and the methods of production [4-6]. In this way, obtaining and using nanocellulose from new lignocellulosic sources increases the possibilities of feedstock and contributes to the development of new materials.

In the literature, nanocellulose, extracted from different plants, are used to reinforce a lot of biodegradable or non-biodegradable matrix in order to improve the properties of nanocomposites. In this context, is possible to highlight nanocomposites such as poly(3-hydroxybutyrate)(PHB)/bacterial cellulose [7], polyvinyl acetate/sisal cellulose whiskers [8], natural rubber/cellulosic nanoparticles of sisal fibers [9], thermoplastic starch/cellulose nanofibrils from wheat straw [10], poly (oxyethylene)/ramie whiskers [11], and pea starch/cellulose whiskers from pea hull fiber [12].

Among the most widely used biodegradable matrices in the production of nanobiocomposites, poly (3-hydroxybutyrate-co-3-hydroxyvalerate) (PHBV) has been widely cited in literature because it is a biodegradable polymer, of natural origin and, with similar physical properties to polyethylene and polypropylene [13, 14]. PHBV is a copolymer of PHB obtained from the addition of 3-hydroxybutyrate and 3-hydroxyvalerate groups (HV), at different concentrations. This monomer is added to the PHB chain with the aim of improving PHB properties such as flexibility and thermal stability, because decrease the melting point, strength and stiffness [3, 15].

Even with the addition of HV, the mechanical and thermal properties of PHBV can be improved with the addition of nanoreinforcements such as nanocellulose, which act as nucleating agents under isothermal crystallization condition [16]. In addition due to bonds between the OH groups of the cellulose nanoparticles, a rigid network is formed, and the transfer of tensile is facilitate and mechanical properties of the polymer matrix is increased [17].

In the present work, the nanocellulose used was obtained from the *Imperata Brasiliensis* (IB) fibers, a plant not explored in the literature for this purpose, and that was successfully used to obtain nanocellulose in the work of BENINI [18]. In this way, the capacity of CNFs strengthening, obtained from the IB fibers shall be studied in order to verify the feasibility of using a specific type of grass to improve some properties of the PHBV.

Currently, biodegradable nanocomposites are obtained using different manufacturing processes and the determination of the most suitable method depends upon the required properties. In the literature, the most widespread process is the solvent evaporation samples obtained by solution casting, which allows obtaining thin films without the use of sophisticated equipment and with a simple and inexpensive process [19]. On the other hand, electrospinning is an attractive technique to produce polymeric fibers in submicron scales, arranged in the form of extremely thin mats [20]. Electrospinning is a simple process, but with many variables, which allows the mats production with specific properties, different from that films obtained by solution casting.

In order to establish the properties of biodegradable nanocomposites and make them more widespread, nanobiocomposites of poly(3-hydroxybutyrate-co-3-hydroxyvalerate) (PHBV) and cellulose nanofibrils (CNFs), extracted from *Imperata brasiliensis* fibers, were obtained by electrospinning and solution casting and evaluated according to their physical and thermal properties.

## 2. MATERIALS AND METHODS

### 2.1 Materials

*Imperata brasiliensis* (IB) fibers used in the present work were gathering from Guaratinguetá at São Paulo state, Brazil [18]. The chemical reagents used were chloroform ( $\text{CHCl}_3$ ) purchase from Dinâmica, sulfuric acid ( $\text{H}_2\text{SO}_4$ , 98%), sodium hydroxide (NaOH) and dimethylformamide ( $\text{C}_3\text{H}_7\text{NO}$ ) (DMF) from Sigma-Aldrich, hydrogen peroxide ( $\text{H}_2\text{O}_2$ , 30%) from Vetec and cellulose membrane dialysis tubing (MWCO 12000- 14000) from Servapor®.

Polymeric matrix used as a matrix were poly (3-hydroxybutyrate-co-3-hydroxyvalerate) (PHBV), kindly supplied by PHB Industrial S/A with the follow properties: molecular weight of 379.160 daltons, 8.71% of PHB-HV, specific weight of 1.230 ( $\text{g}/\text{cm}^3$ ), crystallinity of 44.4% and melting temperature of 167.20 °C.

### 2.2 *Imperata brasiliensis* (IB) hydrolysis

IB fibers were dried in an oven for 48 h at 60 °C, then grounded in a mill and sieved until pass through 25 mesh. The dried fibers were treated with 5 % (w/w) of alkaline solution at 75 °C for 1h under constant mechanical stirring. After that alkali treated fibers were three times bleached with a solution 1:1  $\text{H}_2\text{O}_2$  24 % (v/v) and NaOH 4 % (w/w) for 2 h at 50 °C, under constant mechanical stirring. After each chemical treatment, fibers were filtered and rinsed with distilled water until neutral pH. The treated fibers were subsequently dried in an oven for 48 h at 60 °C.

CNFs were obtained, from bleached fibers, by sulfuric acid hydrolysis using 64 % of  $\text{H}_2\text{SO}_4$  (w/w) during 75 min, with a pulp:solution rate of 1:20 ( $\text{g}/\text{mL}$ ) at 35 °C. After acid hydrolysis suspension was centrifuged at 5000 rpm for 30 min and dialyzed in distilled water until neutral pH. The colloidal suspension was sonicated at 20 kHz of frequency and 750 watts, during 5 min in ice-bath and then dried in a conventional oven at 30 °C until total water evaporation.

### 2.3 Nanocomposites obtaining

PHBV (5 % in relation to solvent weight) was solubilized in a mixture of solvents according to the following conditions: solvent ratio of DMF:  $\text{CHCl}_3$  (22:78) at 50 °C for 30 h in a closed system, with condenser.

For nanocomposite process, 1% (w/w) of dried CNFs, with respect to PHBV weight, were mixed with DMF. CNFs/DMF suspension was sonicated in an ultrasound Sonics & Materials (model VCX 750), at 20 kHz of frequency and 750 watts, with pulses of 20 s with 5 s at rest, 25 % of amplitude, during 60 min.

CNFs/DMF suspension was slowly added with dropper to the PHBV/CHCl<sub>3</sub> solution and the system was kept sealed, stirred at 50 °C until complete solubilization time of 30 h, according to scheme shown in Figure 1.

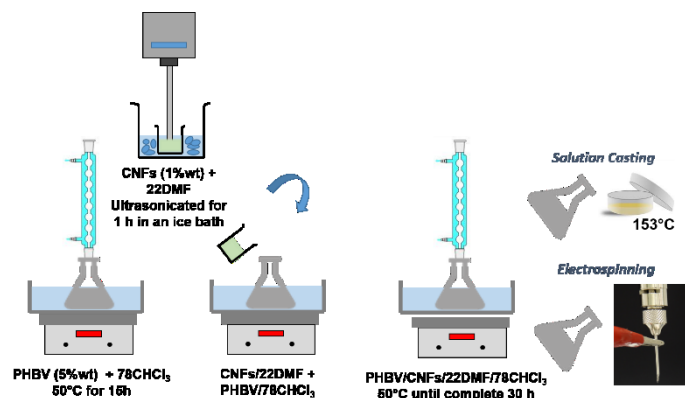


**Figure 1:** Scheme of nanocomposites production.

Then, PHBV and nanobiocomposites solutions were poured into a petri dish to obtain films by solution casting (PHBVc and PHBV/CNFsc) and mats by electrospinning (PHBVe and PHBV/CNFse).

Films were obtained using drying casting temperature of 153 °C and mats were obtained according to the following electrospinning parameters: needle 20x10, drum collector rotation 27 rpm, working distance of 10 cm with environmental conditions close to 25 °C and 50 % humidity. PHBVe and PHBV/CNFse mats were electrospun for 25 min and 35 min, respectively.

#### 2.4 Films and mats characterization

Surface of electrospinning mats and casting films were analyzed as obtained, without further preparation, by a JEOL JSM5310 scanning electron microscope with a tungsten filament operating at 20 kV, utilizing a low vacuum technique and working distance of 12 mm. All samples were coated with gold thin layer to make them conductive before the SEM analysis.

Diffractiongrams were carried out on a Shimadzu diffractometer (XDR-6000 model), operating at 40 kV, 30 mA and CuK $\alpha$  radiation ( $\lambda = 0.1542$  nm). Samples were scanned in  $2\theta$  ranges varying from 10 to 30° (2 $\theta$ /5 s). The values of *d*-spacing and crystallite size (*L*) for the two main crystalline planes (020) and (110) were evaluated as well the total crystallinity index (CI). Initially, deconvolution of the peaks was performed to check the contribution of each crystalline plane. The *d*-spacing of each plane was calculated using Bragg's equation and the crystallite size was calculated using the Scherrer's equation [21]. The CI index was calculated according to the Ruland's method [22].

Differential scanning calorimetry (DSC) thermal analysis were carried out in a Perkin Elmer equipment, model 8000. Analyses were performed under nitrogen atmosphere with a heating rate of 10 °C/min and cooling at 30 °C/min. The first heating was carried out in order to remove the thermal history of the sample (-50 °C to 220 °C). The temperatures and enthalpies of fusion and crystallization were calculated from the maximum and the peak area of the second heating curve, respectively.

The measurements of the films and mats thickness were carried out with a micrometer and represent the mean of three values.

### 3. RESULTS AND DISCUSSIONS

Using solution casting and electrospinning techniques, thin films and mats of PHBV and PHBV/CNFs were obtained, as shown in Figure 2. The thickness of the films obtained by casting was  $93.33 \pm 5.77$   $\mu$ m while nanocomposites obtained by electrospinning presented  $40.00 \pm 10.00$   $\mu$ m.

In the visual analysis of the casting films it was not observed the presence of agglomerates, due to homogeneous aspect, also transparency was not affected by CNFs addition, indicating that the used method to mix CNFs with PHBV matrix was efficient. This same behavior was observed in the study of SILVERIO, *et al.* [23] for the incorporation of cellulose nanocrystals from corncobs in PVA (polyvinyl alcohol) matrix. In the mats obtained by electrospinning, it is possible to observe that there is no difference in the visual

aspect of the pure polymer and nanocomposite.

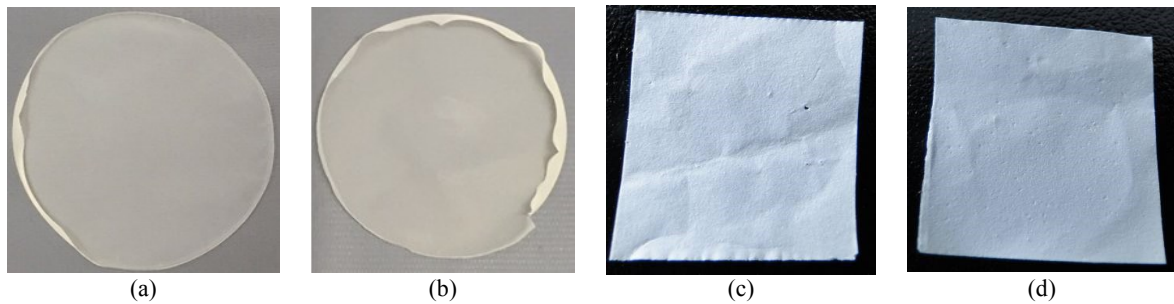


**Figure 2:** Films obtained by solution casting (a) PHBVc, (b) PHBV/CNFsc; mats obtained by electrospinning (c) PHBVe and (d) PHBV/CNFse.

Materials obtained by electrospinning are completely different from those obtained by solution casting. Using solution casting were produced transparent and homogeneous films, easily demolded from the surface on which they were obtained (petri dish), while by electrospinning process, extremely thin and flexible mats were obtained with a white color, opacity, and adhered to the surface on which were electrospinning (aluminum foil).

Nanocomposites obtained by solution casting and electrospinning were also analyzed by SEM (Figure 3) in order to observe the uniformity of the reinforcement on the polymeric matrix and also the uniformity of microfibers and the presence of some defects.

In the SEM images of the nanocomposites casting film (Figure 3a), there is a homogeneous surface, without the visible presence of agglomerates. Some pores were caused by the fast evaporation of the solvent due to the high volatility during the drying process at 153 °C [24].

SEM images of electrospinning mat, shown in Figure 3b, revealed a homogeneous morphology without the presence of beads, indicating that the addition of CNFs in the polymer solution improved the electrospinning process, because addition of CNFs tends to increase the viscosity of the solution, which decreases droplet formation at the needle tip, preventing the formation of beads. Also, addition of CNFs increase the time of electrospinning (in 10 min), which was limited according to solution properties.

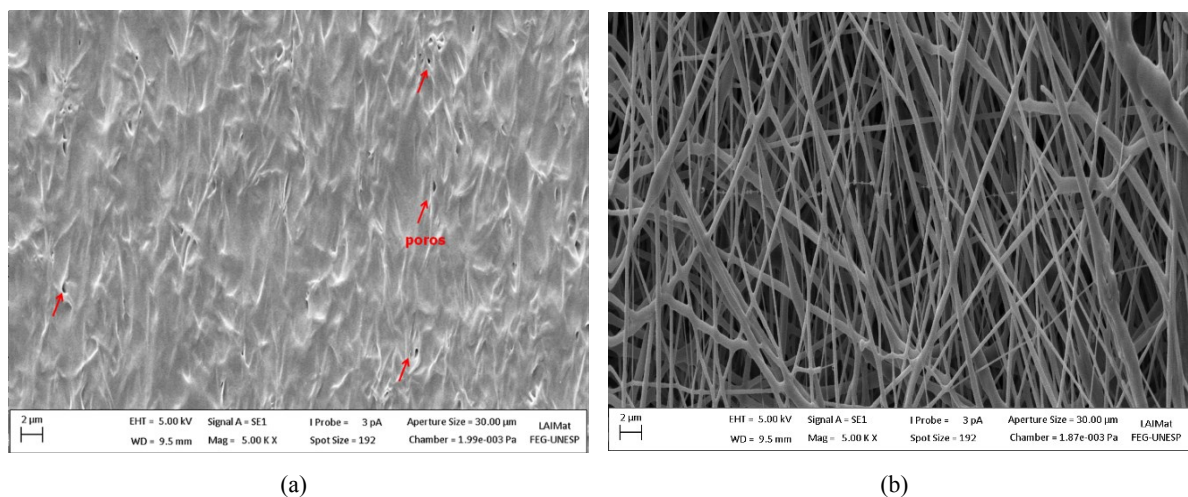


**Figure 3:** SEM of nanocomposites (a) PHBV/CNFsc and (b) PHBV/CNFse.

With the SEM images, the values of the average diameter of the polymer fibers in the electrospinning mats were determined. The histograms with the fiber diameter distribution are shown in Figure 4.

For the pure PHBV, as seen in Figure 4a, the diameter of the fibers varied between 0.08  $\mu\text{m}$  and 0.53  $\mu\text{m}$ , whereas for the nanocomposite (Figure 4b) this variation was between 0.13  $\mu\text{m}$  and 0.76  $\mu\text{m}$ . The mean diameter of the fibers in the PHBV mat was 0.20  $\mu\text{m}$ , whereas for the nanocomposite was 0.37  $\mu\text{m}$ .

With analyze of the graph in Figure 5, it can be seen that the addition of the CNFs provided a significant increase in the diameter of the fibers, which may be due to the increase in the viscosity of the solutions. However, considering the standard deviation values, which were close for all samples, there is no statistically significant difference between the diameter values.

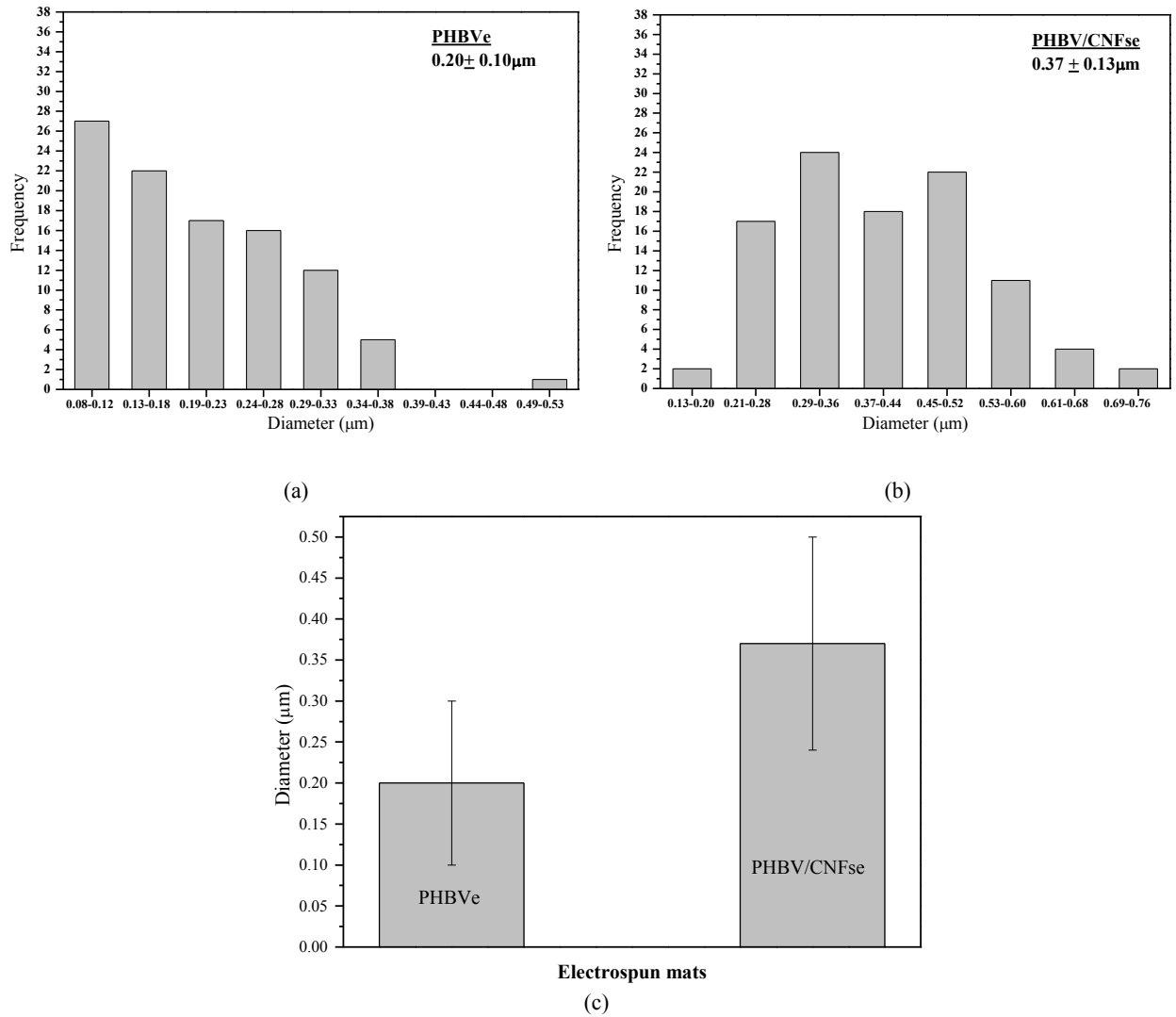


**Figure 4:** Distribution of fiber diameter values in electrospun mats (a) PHBV and (b) PHBV/CNFse, and distribution of fiber diameter values in electrospun mats.

To evaluate the effect of CNFs addition on the PHBV crystallinity properties, films and mats were characterized by X-ray diffraction (XRD) and the curves are shown in Figure 6.

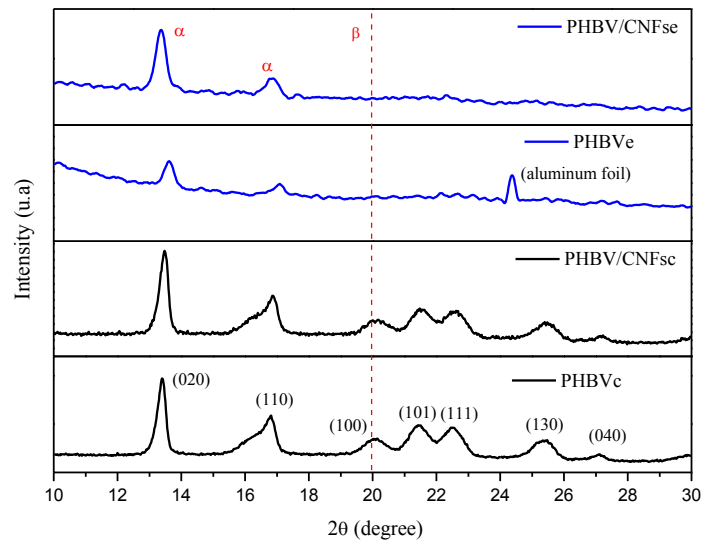


**Figure 6:** XRD of PHBV and nanocomposites obtained by solution casting and electrospinning.

The XRD patterns of the films obtained by solution casting showed two main diffraction peaks, which are typical of an orthorhombic crystal structure of PHB (crystals  $\alpha$ ) in  $2\theta \approx 13.4^\circ$  and  $16.8^\circ$  relative to crystallographic planes (020) and (110), and a diffraction peak of hexagonal crystalline structure (crystals  $\beta$ ) in  $2\theta \approx 20.0^\circ$ . The other peaks in  $2\theta$  near to  $21.4^\circ$ ;  $22.5^\circ$ ;  $25.4^\circ$  and  $27.1^\circ$ , are related to crystallographic planes (100), (101), (111), (130) and (040), respectively [25]. Diffractograms of electrospinning materials presented only two crystalline peaks, near to  $2\theta \approx 13^\circ$  and  $17^\circ$ , due to crystallographic planes (020) and (110), respectively, showing that electrospinning changes the crystalline structure of materials.

Table 1 presents the main crystallinity parameters determined from XRD curves. Addition of CNFs in nanocomposites obtained by solution casting, did not interfere in the values of *d-spacing*, however, provided a slight increase in the crystallite size (L) perpendicular to the planes (110), with a consequent reduction in the crystallinity index (CI).

**Table 1:** Crystallinity parameters of PHBV and its nanocomposites.

PROPERTIES	<i>D-SPACING</i> (nm)		L (nm)		CI (%)
	020	110	020	110	
PHBVc	0.661	0.526	27.887	13.124	73.0
PHBV/CNFsc	0.657	0.526	26.990	14.736	64.4
PHBVe	0.649	0.519	28.857	33.609	68.4
PHBV/CNFse	0.639	0.527	25.351	19.090	56.0

For electrospinning materials, values of crystallites size (L) showed a slight reduction in the plane (020) and a significant reduction in the plane (110), when compared to pure PHBV. Although the electrospinning process inhibits crystal formation in other planes, CNFs acts more effectively as nucleating agents, as evinced by the reduction in the crystallite size; however, it also led to a significant reduction the CI values. In addition, regarding the electrospinning results, it is possible to state that the peak relative to the substrate in which the mats were obtained (aluminum foil) did not appear for the nanocomposites, indicating a greater thickness of these mats, due to the longer process time.

The DSC curves of the second heating for PHBV and their nanocomposites obtained by solution casting and electrospinning are shown in Figure 7.

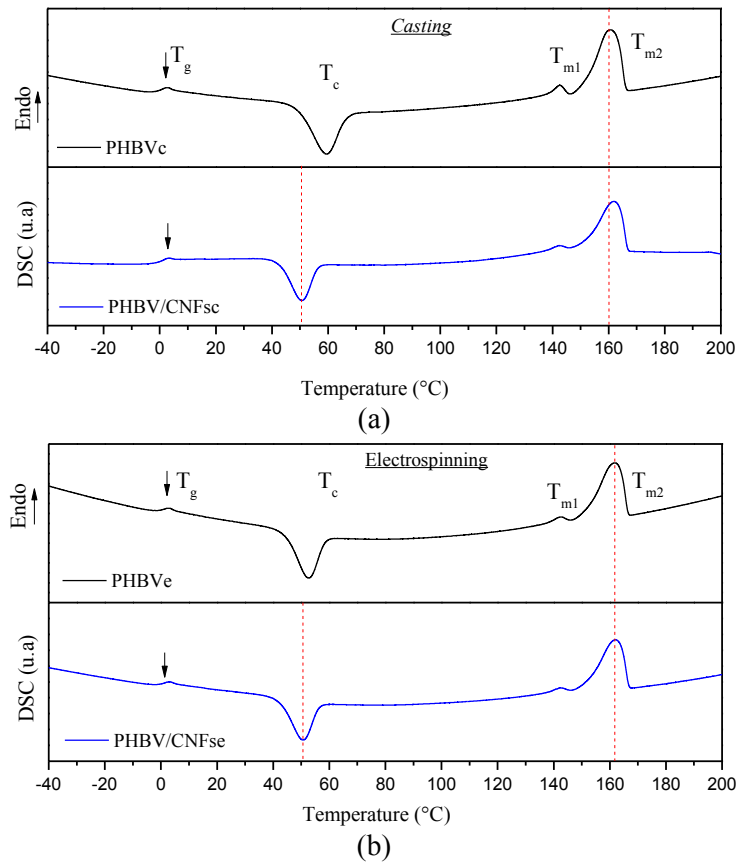


**Figure 7:** DSC curves of 2nd heating for PHBV and PHBV/CNFs by (a) casting and (b) electrospinning.

The values of glass transition temperature ( $T_g$ ), crystallization temperature ( $T_c$ ), crystalline melting temperature ( $T_m$ ), and the melting ( $\Delta H_{m1}/\Delta H_{m2}$ ) and crystallization ( $\Delta H_c$ ) enthalpy, which are described in Table 2, were obtained from these graphs. All samples presented, in the second heating, glass transition temperature ( $T_g$ ) between 0.1 and 0.4 °C, one exothermic peak of crystallization and two endothermic melting peaks.

**Table 2:** Thermal parameters of PHBV and its nanocomposites.

PROPERTIES	$T_g$ (°C)	$T_c$ (°C)	$\Delta H_c$ (J/g)	$T_{m1}/T_{m2}$ (°C)	$\Delta H_{m1}/\Delta H_{m2}$ (J/g)
PHBVc	0.1	59.2	41.2	142.8/161.2	2.7/48.4
PHBV/CNFsc	0.1	46.5	12.9	142.9/162.2	2.1/44.4
PHBVe	0.3	52.6	36.5	141.9/162.2	4.7/49.8
PHBV/CNFse	0.4	50.4	36.2	142.2/162.1	2.0/50.4

The glass transition temperatures of the nanocomposites showed no significant changes compared to that of the pure polymer. The same behavior was observed for PHBV nanocomposites reinforced with 1, 2, 3, 4 and 5% (w/w) of nanocellulose in the work of TEN, *et al.* [26], which could indicate that independent of the cellulose content, the presence of these nanocrystals does not significantly interfere in the PHBV glass transition temperature. However, addition of the CNFs, decreased the  $T_c$  and  $\Delta H_c$ , in special for films obtained by solution casting, indicating that CNFs acts as a nucleating agent for PHBV. The same behavior was observed in the study of JIANG, *et al.* [3] and TEN, *et al.* [26] which stated that the CNFs acts as nucleating agent, and induces PHBV to crystallize at lower temperatures, since it reduces the energy barrier for the formation of PHBV nucleus. The presence of a crystallization peak in the cooling curve of the PHBV/CNFsc ( $T_c = 53.8$  °C and  $\Delta H_c = 15.9$  J/g) explains the lower values of  $T_c$  and  $\Delta H_c$ , obtained in the 2nd heating, whereas for the other samples, no thermal event occurred during cooling.

For electrospun nanocomposites, CNFs also caused a reduction in  $T_c$  of 2.2 °C, but this reduction was less pronounced since materials obtained by this process showed loss of some crystal planes. All samples, casting and electrospinning, showed two endotherms peaks with melting temperatures ranging from 142.2 °C to 142.9 °C for  $T_{m1}$ , and between 161.2 °C and 162.2 °C, for  $T_{m2}$ .

Ten et al. [26] relates these two melting peaks to fusion-melting-recrystallization process of the polymer, on the other hand according to Del Gaudio *et al.* [27] this two melting peaks are reported in the literature as the fusion of the primary crystals and recrystallized material. In general, the addition of the CNFs has not caused significant changes in the values of melting temperatures. On the other hand, the size of the first melting peak,  $\Delta H_{m1}$  values, was reduced with the addition of the CNFs, indicating that the presence of the reinforcement inhibited the formation of defective crystals, which melt at lower temperatures.

In the first heating curves the glass transition and crystallization events was not observed, as well as the first melting peak, indicating that all samples were fully crystallized during the casting process and/or electrospinning [26]

#### 4. CONCLUSIONS

PHBV/CNFs nanobiocomposites were obtained by solution casting and electrospinning process. Films and mats presented different properties since that electrospinning changed the crystalline structure of PHBV matrix. For nanobiocomposites obtained by solution casting, addition of 1% (w/w) CNFs did not affected the films transparency and visual appearance, but provided a significant increase in the crystallization rate, with a consequent reduction in the crystallinity index. For electrospinning nanobiocomposites changes in the crystallization rate was less effective, on the other hand, a considerable improvement in process efficiency, with increasing electrospinning time resulting in better mats quality, was observed.

#### 5. ACKNOWLEDGMENTS

The authors acknowledge FAPESP (2011/14153-8) and Capes for fellowships and financial support.

#### 6. BIBLIOGRAPHY

- [1] ABDUL KHALIL, H.P.S., BHAT, A.H., IREEANA YUSRA, A.F., "Green composites from sustainable cellulose nanofibrils: A review", *Carbohydrate Polymers*, v. 87, n. 2, pp. 963-979, Jan. 2012.
- [2] DUFRESNE, A. "Cellulose nanomaterial reinforced polymer nanocomposites", *Current Opinion in Colloid&Interface Science*, v. 29, pp.1-8, 2017.
- [3] JIANG, L., MORELIUS, E., ZHANG, J., et al., "Study of the Poly(3-hydroxybutyrate-co-3-hydroxyvalerate)/Cellulose nanowhisker composites prepared by solution casting and melt processing", *Journal of Composites Materials*, v. 42, pp.2629-2645, 2008.
- [4] ZHAO, J., ZHANG, W., ZHANG, X., et al., "Extraction of cellulose nanofibrils from dry softwood pulp using high shear homogenization", *Carbohydrate Polymers*, v. 97, pp. 695-702, Set. 2013.
- [5] PAAKKO, M., AHOLA, S., "Enzymatic Hydrolysis Combined with Mechanical Shearing and High-Pressure Homogenization for Nanoscale Cellulose Fibrils and Strong Gels", *Biomacromolecules*, v. 8, n. 6, pp.1934-1941, 2007.
- [6] QUA, E. H., HORNSBY, P. R., SHARMA, H. S. S., et al., "Preparation and characterisation of cellulose nanofibers", *Journal of Materials Science*, v. 46, pp. 6029-6045, 2011.
- [7] BARUD, H. S., SOUZA, J. L., SANTOS, D. B., et al., "Bacterial cellulose / poly (3-hydroxybutyrate) composite membranes", *Carbohydrate Polymers*, v. 83, n. 3, pp.1279-1284, 2011.
- [8] GARCIA DE RODRIGUEZ, N. L., THIELEMANS, W., DUFRESNE, A., "Sisal cellulose whiskers reinforced polyvinyl acetate nanocomposites", *Cellulose*, v. 13, n. 3, pp. 261-270, 2006.
- [9] SIQUEIRA, G., TAPIN-LINGUA, S., BRAS, J., et al., "Mechanical properties of natural rubber nanocomposites reinforced with cellulosic nanoparticles obtained from combined mechanical shearing, and enzymatic and acid hydrolysis of sisal fibers", *Cellulose*, v. 18, n. 1, pp. 57-65, 2011.
- [10] KAUSHIK, A., SINGH, M., VERMA, G., "Green nanocomposites based on thermoplastic starch and steam exploded cellulose nanofibrils from wheat straw", *Carbohydrate Polymers*, v. 82, n. 2, pp. 337-345, 2010.
- [11] ALLOIN, F., D'APREA, A., DUFRESNE, A., et al., "Poly(oxyethylene) and ramie whiskers based nanocomposites: Influence of processing: Extrusion and casting/evaporation", *Cellulose*, v. 18, n. 4, pp. 957-

973, 2011.

- [12] CHEN, Y., LIU, C., CHANG, P. R., CAO, X., *et al.*, “Bionanocomposites based on pea starch and cellulose nanowhiskers hydrolyzed from pea hull fibre: Effect of hydrolysis time”, *Carbohydrate Polymers*, v. 76, n. 4, 607–615, 2009.
- [13] CARLI, L. N., CRESPO, J. S., MAULER, R. S., “PHBV nanocomposites based on organomodified montmorillonite and halloysite: The effect of clay type on the morphology and thermal and mechanical properties”, *Composites Part A*, v. 42, n. 11, pp. 1601–1608, 2011.
- [14] KE, Y., ZHANG, X. Y., RAMAKRISHNA, S., *et al.*, “Reactive blends based on polyhydroxyalkanoates: Preparation and biomedical application”, *Materials Science and Engineering C*, v.70, pp. 1107–1119, 2017.
- [15] MOFOKENG, J. P., LUYT, A. S., “Morphology and thermal degradation studies of melt-mixed PLA/PHBV biodegradable polymer blend nanocomposites with TiO<sub>2</sub> as filler”, *Journal of Applied Polymer Science*, v. 42138, pp. 1–11, 2015.
- [16] KASHANI RAHIMI, S., OTAIGBE, J. U., “The role of particle surface functionality and microstructure development in isothermal and non-isothermal crystallization behavior of polyamide 6/cellulose nanocrystals nanocomposites”, *Polymer*, v. 107, pp. 316–331, 2016.
- [17] MANDAL, A., CHAKRABARTY, D., “Studies on the mechanical, thermal, morphological and barrier properties of nanocomposites based on poly (vinyl alcohol) and nanocellulose from sugarcane bagasse”, *Journal of Industrial and Engineering Chemistry*, v. 20, pp. 462–473, 2014.
- [18] BENINI, K.C.C.C., *Compósitos de nanocelulose/PHBV: manta microfibrilica por eletrofiação*, Tese de D.Sc., FEG/UNESP, Guaratinguetá, SP, Brasil, 2015.
- [19] SIQUEIRA, G., BRAS, J., DUFRESNE, A., “Cellulosic Bionanocomposites: A review of preparation, properties and applications”, *Polymers*, v. 2, pp. 728-765, 2010.
- [20] TIAN, L., ZI-QIANG, S., JIAN-QUAN, W., *et al.*, “Fabrication of hydroxyapatite nanoparticles decorated cellulose triacetate nanofibers for protein adsorption by coaxial electrospinning”, *Chemical Engineering Journal*, v. 260, pp. 818-825, 2015.
- [21] ORNAGHI, H. L., JR., ZATTERA, A. J., AMICO, S. C., “Thermal behavior and the compensation effect of vegetal fibers”, *Cellulose*, v. 21, pp. 189–201, 2014.
- [22] MACEDO, J.S., *Desenvolvimento de biocompósitos à base de polihidroxitirato e resíduos do processamento de fibras de casca de coco*, Tese de D.Sc., COPPE - Universidade Federal do Rio de Janeiro, Rio de Janeiro, RJ, Brasil, 2010.
- [23] SILVÉRIO, H.A., FLAUZINO NETO, W.P., DANTAS, N.O., *et al.*, “Extraction and characterization of cellulose nanocrystals from corn cob for application as reinforcing agent in nanocomposites”, *Industrial Crops and Products*, v. 44, pp. 427-436, 2013.
- [24] MARTÍNEZ-SANZ, M., VILLANO, M., C., OLIVEIRA, M.G.E., *et al.*, “Characterization of polyhydroxyalkanoates synthesized from microbial mixed cultures and of their nanobiocomposites with bacterial cellulose nanowhiskers”, *New Biotechnology*, v. 00, pp.1-3, 2013.
- [25] WANG, C., HSU, C., HWANG, I., “Scaling laws and internal structure for characterizing electrospun poly [(R)-3-hydroxybutyrate] fibers”, *Polymer*, v. 49, pp. 4188–4195, 2008.
- [26] TEN, E., TURTLE, J., BAHR, D., *et al.*, “Thermal and mechanical properties of poly(3-hydroxybutyrate-co-3-hydroxyvalerate) / cellulose nanowhiskers composites”, *Polymer*, v. 51, pp. 2652-2660, 2010.
- [27] DEL GAUDIO, ERCOLANI, C., E., NANNI, F., *et al.*, “Assessment of poly(e-caprolactone)/poly(3-hydroxybutyrate-co-3-hydroxyvalerate) blends processed by solvent casting and electrospinning”, *Materials Science and Engineering A*, v. 528, pp. 1764-1772, 2012.